



---

**Development of Ordered Nanocomposites through the use of Block Copolymer Self-Assembly and Additive Manufacturing**

**Daniel Krogstad  
UNIVERSITY OF ILLINOIS**

---

**08/07/2020  
Final Report**

**DISTRIBUTION A: Distribution approved for public release.**


**Air Force Research Laboratory  
AF Office Of Scientific Research (AFOSR)/ RTA1  
Arlington, Virginia 22203  
Air Force Materiel Command**

DISTRIBUTION A: Distribution approved for public release.

<b>REPORT DOCUMENTATION PAGE</b>		<i>Form Approved</i> OMB No. 0704-0188
<p>The public reporting burden for this collection of information is estimated to average 1 hour per response, including the time for reviewing instructions, searching existing data sources, gathering and maintaining the data needed, and completing and reviewing the collection of information. Send comments regarding this burden estimate or any other aspect of this collection of information, including suggestions for reducing the burden, to Department of Defense, Executive Services, Directorate (0704-0188). Respondents should be aware that notwithstanding any other provision of law, no person shall be subject to any penalty for failing to comply with a collection of information if it does not display a currently valid OMB control number.</p> <p><b>PLEASE DO NOT RETURN YOUR FORM TO THE ABOVE ORGANIZATION.</b></p>		
<b>1. REPORT DATE (DD-MM-YYYY)</b> 19-08-2020	<b>2. REPORT TYPE</b> Final Performance	<b>3. DATES COVERED (From - To)</b> 01 Feb 2017 to 31 Jan 2020
<b>4. TITLE AND SUBTITLE</b> Development of Ordered Nanocomposites through the use of Block Copolymer Self-Assembly and Additive Manufacturing	<b>5a. CONTRACT NUMBER</b>	
	<b>5b. GRANT NUMBER</b> FA9550-17-1-0128	
	<b>5c. PROGRAM ELEMENT NUMBER</b> 61102F	
<b>6. AUTHOR(S)</b> Daniel Krogstad	<b>5d. PROJECT NUMBER</b>	
	<b>5e. TASK NUMBER</b>	
	<b>5f. WORK UNIT NUMBER</b>	
<b>7. PERFORMING ORGANIZATION NAME(S) AND ADDRESS(ES)</b> UNIVERSITY OF ILLINOIS 506 S WRIGHT STREET SUITE 364 URBANA, IL 61801-3649 US		<b>8. PERFORMING ORGANIZATION REPORT NUMBER</b>
<b>9. SPONSORING/MONITORING AGENCY NAME(S) AND ADDRESS(ES)</b> AF Office of Scientific Research 875 N. Randolph St. Room 3112 Arlington, VA 22203		<b>10. SPONSOR/MONITOR'S ACRONYM(S)</b> AFRL/AFOSR RTA1
		<b>11. SPONSOR/MONITOR'S REPORT NUMBER(S)</b> AFRL-AFOSR-VA-TR-2020-0142
<b>12. DISTRIBUTION/AVAILABILITY STATEMENT</b> A DISTRIBUTION UNLIMITED: PB Public Release		
<b>13. SUPPLEMENTARY NOTES</b>		
<b>14. ABSTRACT</b> Hierarchically ordered materials have wide-ranging potential benefits through improved mechanical properties and controllable optical, thermal and/or electronic properties. To achieve this level of control, a combined bottom-up and top-down approach to materials assembly is needed. Here, we report progress towards this goal by studying the self-assembly, rheology and thermal characteristics of 30 printable block copolymer (BCP)-containing epoxy inks. We have identified three different BCPs that can self-assemble in an epoxy/ionic liquid system that can be printed using direct ink writing (DIW). In this way, the BCPs can direct the bottom-up assembly, while DIW can be used for top-down assembly. Interestingly, we have shown that the SCP-containing inks actually have more favorable rheological properties compared to the base inks. Through this work, we identified transient creep testing as an important rheological characterization method that more directly correlates to the printing process. Lastly, we studied the structural evolution of the BCPs during epoxy curing. We have shown that the samples can be heated to 60 C for several hours without appreciable epoxy crosslinking. While this temperature proved insufficient for significant thermal annealing of the BCP microstructure, it may be helpful to alter the rheology and subsequent printability of the inks. Additionally, we showed that the BCP micelles do not dissociate in the ink during epoxy crosslinking, but the structures do change significantly. Typically, they transition from disordered to higher ordered structures, however these exact ordering mechanisms are still unknown. Overall, this project has greatly increased our knowledge of how these materials behave and sets the stage for further development of hierarchically ordered nanocomposites.		
<b>15. SUBJECT TERMS</b> block copolymer self-assembly, direct ink printing, hybrid materials		

Standard Form 298 (Rev. 8/98)  
Prescribed by ANSI Std. Z39.18

DISTRIBUTION A: Distribution approved for public release.

16. SECURITY CLASSIFICATION OF:			17. LIMITATION OF ABSTRACT	18. NUMBER OF PAGES	19a. NAME OF RESPONSIBLE PERSON
a. REPORT	b. ABSTRACT	c. THIS PAGE			PAN, MING-JEN
Unclassified	Unclassified	Unclassified	UU		<b>19b. TELEPHONE NUMBER</b> (Include area code) 703-696-7343 

# Development of Ordered Nanocomposites through the use of Block Copolymer Self-Assembly and Additive Manufacturing

Final Report

FA9550-17-1-0128

Daniel Krogstad

University of Illinois at Urbana-Champaign

## Abstract

Hierarchically ordered materials have wide-ranging potential benefits through improved mechanical properties and controllable optical, thermal and/or electronic properties. To achieve this level of control, a combined bottom-up and top-down approach to materials assembly is needed. Here, we report progress towards this goal by studying the self-assembly, rheology and thermal characteristics of 3D printable block copolymer (BCP)-containing epoxy inks. We have identified three different BCPs that can self-assemble in an epoxy/ionic liquid system that can be printed using direct ink writing (DIW). In this way, the BCPs can direct the bottom-up assembly, while DIW can be used for top-down assembly. Interestingly, we have shown that the BCP-containing inks actually have more favorable rheological properties compared to the base inks. Through this work, we identified transient creep testing as an important rheological characterization method that more directly correlates to the printing process. Lastly, we studied the structural evolution of the BCPs during epoxy curing. We have shown that the samples can be heated to 60 °C for several hours without appreciable epoxy crosslinking. While this temperature proved insufficient for significant thermal annealing of the BCP microstructure, it may be helpful to alter the rheology and subsequent printability of the inks. Additionally, we showed that the BCP micelles do not dissociate in the ink during epoxy crosslinking, but the structures do change significantly. Typically, they transition from disordered to higher ordered structures, however these exact ordering mechanisms are still unknown. Overall, this project has greatly increased our knowledge of how these materials behave and sets the stage for further development of hierarchically ordered nanocomposites.

## Project Motivation

Hierarchical nanocomposites hold great promise for a wide range of applications due to the unique combinations of the mechanical, thermal, electrical, magnetic and/or optical properties that are theoretically possible. However, current fabrication limitations prevent us from taking full advantage of these materials. In order to unlock the potential of these materials, the nanoparticles (NPs) would need to be placed on regular lattices- the exact structure would be determined by the materials and the desired properties. However, when NPs are mixed randomly in a polymer, they are poorly dispersed and are often aggregated which greatly diminishes their potential. To overcome these limitations, there has been a lot of work in functionalizing the NPs with ligands or dispersing them in block copolymer (BCP) micelles in order to space out the particles. While this can work over small domain sizes (~10 microns) or two dimensional surfaces, the ordering cannot currently be extended to three dimensional macrostructures. Therefore, the aim of this project was to investigate the potential to use a combined top-down, bottom-up approach to form hierarchical order from the nanoscale to the macroscale (Figure 1). Specifically, we looked to use BCPs to form an ordered lattice over tens of microns. Then, we could use the shear inherent to direct ink writing (DIW) to align the domains in the print direction, and use the 3D printer to build the

macrostructures. While many parts of this problem had been looked at independently, this was the first known attempt to combine the efforts as a way to create hierarchical nanostructure materials.

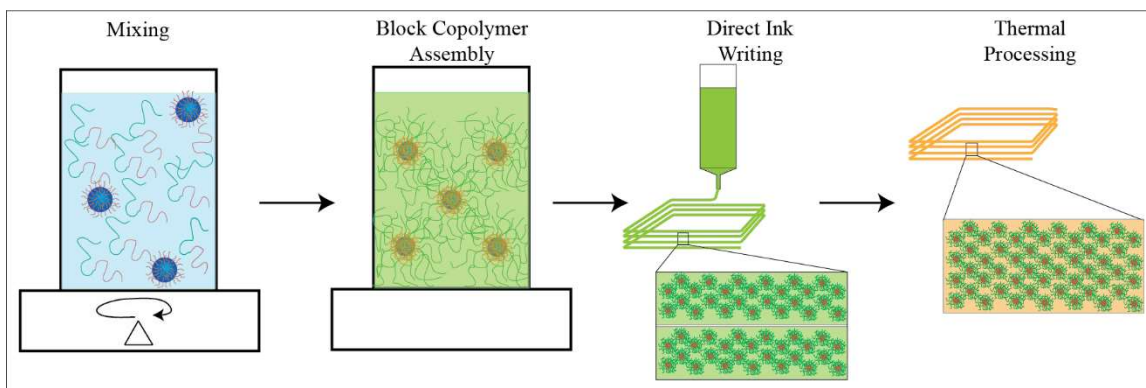


Figure 1: Schematic of the combined top-down, bottom up approach to create hierarchical nanocomposites. First, inks can be created composed of epoxy precursors, block copolymers and NPs. After mixing, the BCPs can self-assemble into ordered nanostructures within the inks. The inks can then be printed in DIW and the shear further aligns the micelles, while the DIW process builds up macroscale components. Thermal processing can further anneal the structures before crosslinking the epoxy.

During the course of this project, three distinct efforts were pursued to push us towards the goal of developing a method to create hierarchically structured epoxies. In the first effort, we needed to identify BCPs that could form ordered structures in a 3D printable resin. In this study, we focused on an interesting 3D printable epoxy ink that has high-temperature and high-strength properties when cured. The second effort consisted of studying the rheology of the structured inks and correlating the rheological properties to the printability of the resins using DIW. Lastly, the effects of temperature were studied to determine whether the micelles dissolved, remained unchanged, or if they could thermally anneal before the epoxy resins could crosslink.

## Results and Discussion

Significant progress was made in understanding BCP self-assembly in epoxy inks, the effects of the micelles on the rheology of the inks and the structural evolution of the BCPs during thermal processing. This section describes the most significant advances that were made throughout the course of this project.

### *BCP Self-Assembly in Epoxy Ink*

Throughout this project, we have been using a previously developed 3D printable epoxy ink<sup>1</sup> that consists of a bisphenol A diglycidyl ether (BADGE) epoxy precursor with a 1-ethyl-3-methylimidazolium dicyanamide (EMIM-DCA) ionic liquid crosslinker (Figure 2). The formulations also contain nanoclay which imparts shear thinning properties to the inks. The major focus of this effort is to identify BCPs that will form ordered nanodomains in these resins.

<sup>1</sup> Compton, B. G.; Lewis, J. A. 3D-Printing of Lightweight Cellular Composites. *Adv. Mater.* 2014, 26, 5930–5935.

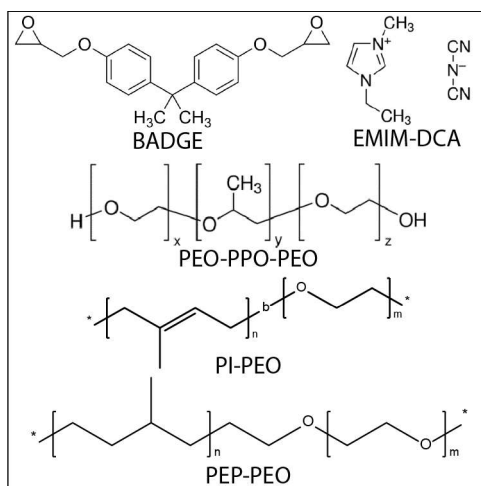


Figure 2: Chemical structures of the ink components.

By definition, block copolymers contain at least two different polymer blocks that are covalently attached to one another. To create nanostructure, these two blocks need to be dissimilar enough that there is an enthalpic driving force to keep them as far apart as possible. In our system, the ideal BCP would have one epoxy-phillic block which is completely dissolved in the solvent (BADGE/EMIM-DCA) and one epoxy-phobic block that wants to completely dissociate from the solvent. In this situation, the dissociating polymer forms the core of phase separated micelles, while the dissolved block extends into the solvent. This configuration results in an overall minimization of the sample free energy. Depending on the block length, and the relative interaction energies of the blocks with the solvent, several different structures can form - ranging from disordered spherical micelles (Sph), spherical micelles aligned on a body centered cubic lattice (BCC), cylindrical micelles aligned on a hexagonal lattice (Hex), a bicontinuous gyroid structure (Gyr) and lamellar domains (Lam) (Figure 3).<sup>2</sup> In our case, we wanted to identify BCPs that could form the ordered BCC and Hex structures at low BCP and EMIM-DCA concentrations. The BCC structure is preferred for optical and mechanical properties, while the Hex configuration is preferred for electrical or thermal conductivity.

<sup>2</sup> Hu, H.; Gopinadhan, M.; Osuji, C. O. Directed Self-Assembly of Block Copolymers: A Tutorial Review of Strategies for Enabling Nanotechnology with Soft Matter. *Soft Matter* 2014, 10, 3867–3889.

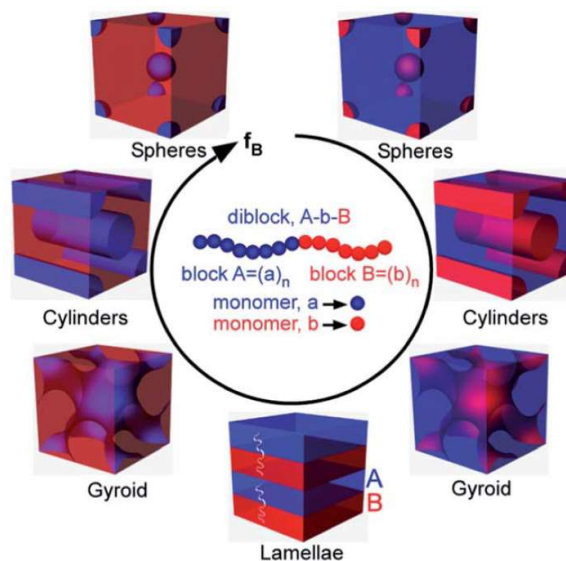


Figure 3: Schematic showing the range of structures that BCP melts can form as a function of the block fraction ( $f_B$ ). Ordered phases include BCC spheres, hexagonally packed cylinders, gyroid and lamellae structures. This figure has been modified from Hu et al.<sup>2</sup> BCPs can form the same range of structures in solvents as well, where one block is miscible in the solvent and one is not.

Over the course of this project, we preliminarily investigated several BCPs including polyethylene oxide-b-polypropylene oxide-b-polyethylene oxide (PEO-PPO-PEO), polyethylene-alt-propylene-b-polyethylene oxide (PEP-PEO), polystyrene-b-polymethyl methacrylate (PS-PMMA) and a novel synthesized polybutyl acrylate-b-polyaminopropylimidazole (PBUA-PIPAA). For the PEO-PPO-PEO polymers, we studied the assembly of several different Pluronic® polymers with varying block lengths. In these polymers, the PEO, PMMA and PIPAA blocks were the epoxy-philic blocks, while the PPO, PEP, PI, PS and PBUA are the epoxy-phobic, nanophase separating blocks.

To determine the self-assembled structure of the BCPs in the epoxy inks, small angle x-ray scattering (SAXS) was used. SAXS was performed both at the Frederick Seitz Materials Research Laboratory (MRL) at Illinois and at the Advanced Photon Source (APS) at Argonne National Laboratory (ANL). During SAXS, a monochromatic beam of x-rays is transmitted through the sample and then collected on a detector. Some small portion of the x-rays scatter off of the nanostructures at very small angles and can be used to determine the shape, spacing and ordering of the self-assembled nanostructures.

From these preliminary investigations, we downselected one PEO-PPO-PEO polymer length (P123), PI-PEO and PEP-PEO as promising BCPs for further investigation (Figure 2). PEO-PPO-PEO did not show extended ordering at low BCP and EMIM-DCA concentrations, but it was selected because it is cheap and available in large quantities so we could make a lot of samples to determine if there is a relevant phase space. PEO-PEP showed significant promise for creating ordered structures. PI-PEO is very similar to PEP-PEO, and is actually a precursor in the synthesis of PEP-PEO. The only difference is PI-PEO retains the carbon-carbon double bond, while the PEP-PEO has been hydrogenated to remove the double bond (Figure 2). The SAXS results on a

wide range of compositions were analyzed to begin to develop ternary phase diagrams of the ink mixtures (Figure 4). In these cases, the PEO blocks are dissolved in the BADGE/EMIM-DCA/nanoclay phase while the other block nanophase separates. For all three BCPs, we identified a range of structures, including regions in which the ordered phases are present. The phases include dissolved polymers with no nanophase separation (Polymer), spherical micelles and three ordered phases: BCC, Hex and Lam structures. These results were a major breakthrough for this effort to show that we can create well ordered nanodomains in the epoxy inks.

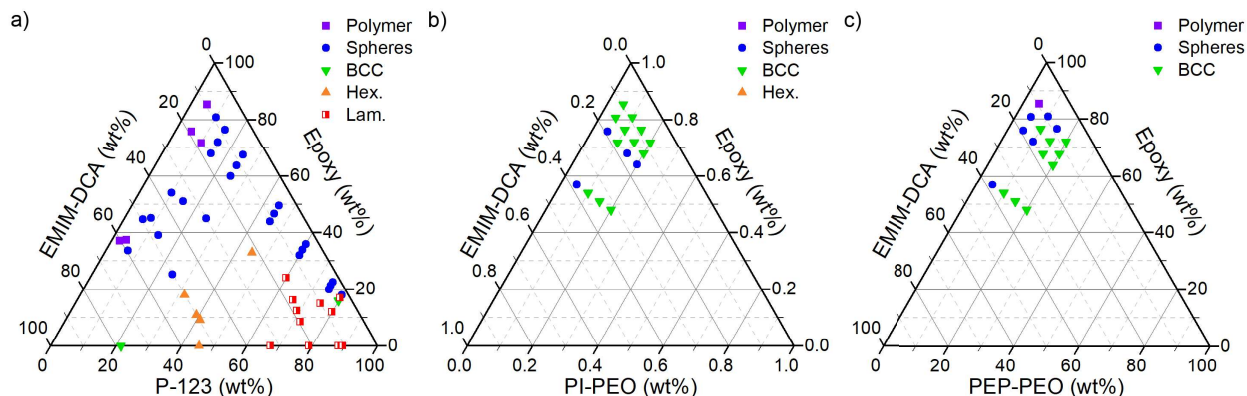


Figure 4: Ternary phase diagrams of the inks showing the internal structure as a function of the epoxy, EMIM-DCA and BCP concentration. a) PEO-PPO-PEO (P-123), b) PI-PEO and c) PEP-PEO. Internal structure present include dissolved polymers (Polymer) disordered spheres (Spheres), Spheres on a BCC lattice (BCC), hexagonally packed cylinders (Hex) and lamellar (Lam) structures.

The PEO-PPO-PEO BCP phase diagram showed results that were consistent with amphiphilic BCPs in a solvent. At the lowest PEO-PPO-PEO concentrations, the polymers were fully dissolved in the solvent (polymer). As the concentration was increased, the disordered spherical micelles were formed in a large phase space. At the highest PEO-PPO-PEO concentrations, both spheres and ordered domains were identified depending on the epoxy/EMIM-DCA concentrations. If the BADGE concentrations were high and EMIM-DCA was low, then the disordered spheres phase formed. The solubility of PPO in BADGE is not that different than the solubility of PEO, which is why the disordered spheres phase dominates at low EMIM-DCA concentrations. In contrast, the solubility of PPO in EMIM-DCA is very poor compared to the solubility of PEO in EMIM-DCA. Therefore, when EMIM-DCA is increased (and the BADGE decreased <35 wt%) (Figure 4a, bottom axis and bottom right corner), then the highly ordered structures (BCC, Hex, Lam) become prevalent. These results indicate that the EMIM-DCA is not only the cross-linking agent in the system, but it is a structure directing agent as well. Unfortunately, these formulations do not form relevant materials due to such low BADGE concentrations.

However, both the PI-PEO and PEP-PEO did form ordered structures at BADGE concentrations of 75 wt% or higher. These formulations can be crosslinked to form high strength materials, and thus are of very strong interest for the development of hierarchically ordered epoxies.

### Resin Printability

The second critical aspect for the development of these systems is understanding how the incorporation of BCPs affects the rheology of the inks. The initial hypothesis for the project was that we could take advantage of the high shear conditions in the DIW to further align the BCP domains through shear annealing. Additionally, the printing allows for the top-down organization

of the tens of microns wide printed lines into macroscale parts and components. Therefore, it is critical to understand the rheology of the inks and how the rheology correlates to printability.

The effect of the BCPs on the epoxy rheology was initially studied using traditional oscillatory rheology tests such as amplitude sweeps and frequency sweeps. Figure 5a shows an example strain amplitude sweep for several inks with varying PEO-PPO concentrations. From these data, it was concluded that the presence of the BCP domains did not significantly change the rheology of the inks: 1) the  $G'$  at low strains are within error of one another, 2)  $G' \gg G''$  at low strains and 3) the yield stress of the inks was equivalent. Together, these results indicate that the ink properties would be roughly equivalent in their ability to support the weight of additional layers, span gaps, and flow with air pressure. However, in our initial printing tests (Figure 5b-c), a higher pneumatic pressure was needed to print consistently with the base ink (850 kPa) than the 20 wt% PEO-PPO ink (700 kPa).

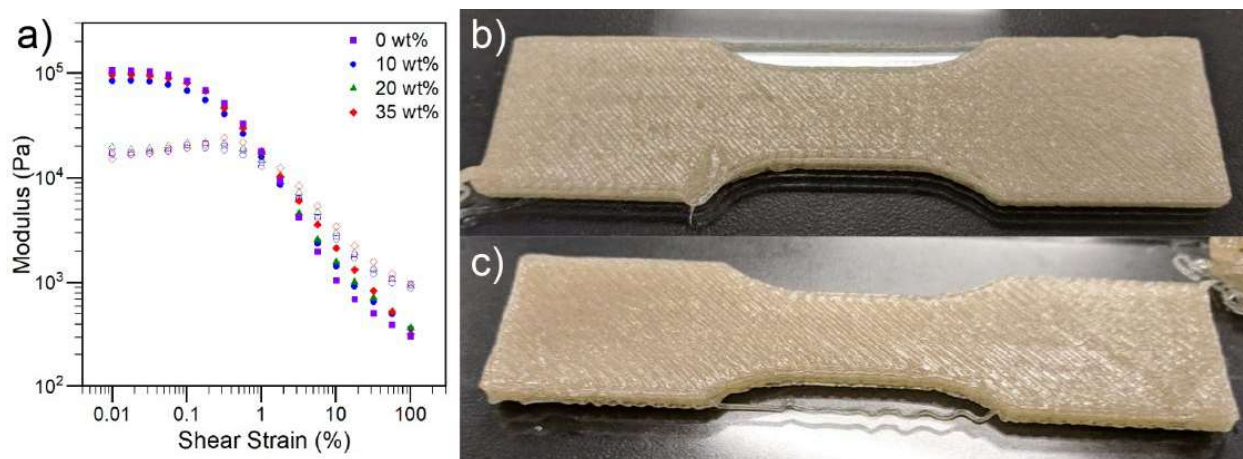


Figure 5: a) Strain amplitude tests for 4 inks with varying PEO-PPO concentrations. These data indicate that the rheological behavior and the yield stress is virtually identical for all 4 formulations. b) Dog bone test prints of the base ink at 850 Pa. c) Dog bone test prints with the 20 wt% PEO-PPO ink at 700 Pa. The base ink required a higher pneumatic pressure in order to print a quality part.

We hypothesized that there were two potential reasons for the discrepancies between the rheology and printing tests. The first, is that the rheological tests are performed in an oscillatory mode, but printing is not oscillatory, it is a continuous flow. While this may not be a problem for many materials, this could be a problem for structured inks such as these since the oscillatory mode can result in a change in the materials structure during each oscillation. The second potential reason is that the time scale of the oscillatory test is not consistent with the time scales of printing. The amplitude sweeps are performed at 1 Hz, meaning that the results correspond to the material response on a time scale of one second or less. Printing, however, could result in shear acting on a material for significantly longer than this. To create equivalent time scales using oscillatory rheology, we would need to characterize the rheology over a wide range of frequencies. No matter which reason is correct, the observed discrepancies showed that the oscillatory amplitude sweeps were not necessarily relevant in assessing the printability of these inks, even though this is the primary method used in the literature.

Instead, we used transient creep experiments to test the rheological properties of the inks. In transient creep testing, a stress is applied to the inks, and the shear rate was measured as a function of time. In this way, we are testing the flow in a linear manner (rather than oscillatory) and at time

scales (up to 5 minutes) that are more consistent with DIW. Transient creep testing has been used to characterize a variety of yield stress fluids, but it has not yet been reported to characterize inks for DIW. The results of the creep tests for the base ink and the 20 wt% PEO-PPO ink can be seen in Figure 6. The data is presented in two ways: first, as the shear rate versus time for a variety of stresses (Figure 6a,c) and second, as the shear stress versus shear rate for a variety of times (Figure 6b,d).

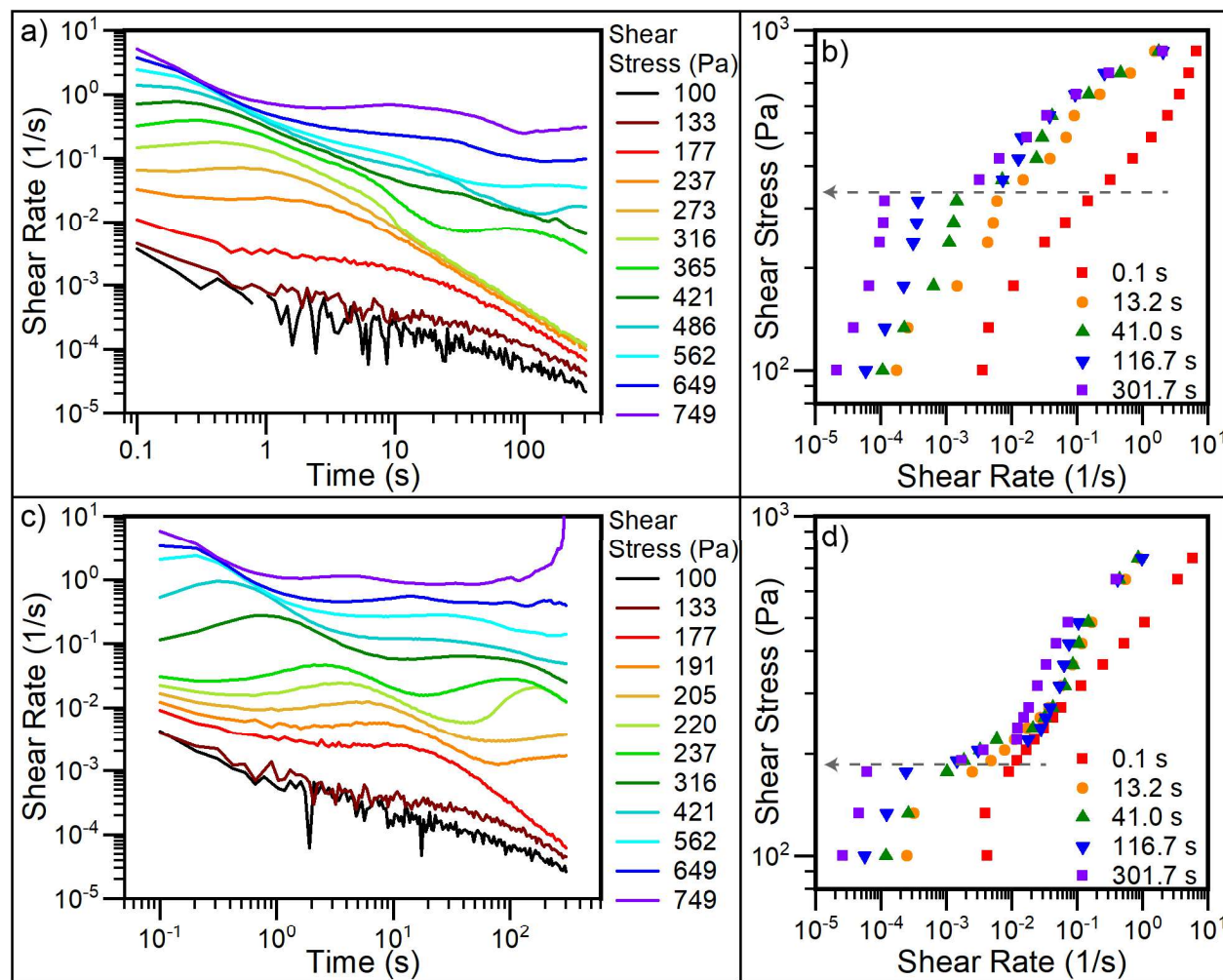


Figure 6: Transient creep testing was performed on a-b) the base ink and c-d) the 20 wt% PEO-PPO ink. a,c) Shear rate versus time was monitored for a wide range of shear stresses. b,d) The shear stress versus shear rate can also be plotted for some example time points to show the flow profile as a function of time. The dashed arrow indicates the yield stress.

From these figures, there are three important conclusions that can be drawn: 1) in both samples, the inks flow well at early time scales, 2) a yield stress eventually emerges and 3) the shear rate data is non-monotonic. Towards the first point, the flow curves (Figure 6b,d) are roughly linear at the earliest time points (0.1s, red squares). However, it is observed that the shear rates generally decrease with time for any given shear stress. This means that the material flow is slowing with time. The second point, is that for both samples, a distinct yield stress emerges for the samples. The yield stress can be observed as a gap in the shear rate vs time plots or as a discontinuity in the flow curves. The arrows in the flow curve plots (Figure 6b,d) show the yield stress for the two

inks, indicating that the yield stress for the base ink is actually higher (365 Pa) and manifests earlier (10 s) than the yield stress for the BCP-containing ink (191 Pa, 50 s). Neither the time dependence of the flow, nor the difference in the emergent yield stresses between the two inks were observable in the oscillatory amplitude sweeps (Figure 5a). The third conclusion was that there were local maxima and minima in the shear rate versus time. This behavior is especially prevalent for the stresses above the yield stress. These behavior are similar to those described previously in the literature for some colloidal yield stress fluids.<sup>3</sup> This previous work has suggested three domains in the material response as a function of the shear stress.

The same data was replotted as the shear rate versus the shear strain to better correlate our data to the results reported by Landrum *et al.*<sup>3</sup> (Figure 7). Plotting the data in this manner shows the same three regions as observed by Landrum *et al.* At the smallest stresses, below the yield stress (Region I), the shear rate decreases as the strain increases indicating a solid-like behavior. In an intermediate regime (Region II), the shear rate is non-monotonic and is said to relate to where the material yields (increase from a local minima), flows (nearly steady shear rate), and later resolidifies (decrease in shear rate) into what is referred to as a re-entrant solid. At high stresses, greater than some critical flow stress (Region III), the inks appear to flow continuously. A comparison of the plots for the base ink and 20 wt% PEO-PPO ink show that there is a significantly more pronounced re-entrant solid regime for the 20 wt% PEO-PPO ink. Additionally, it is unclear if the base ink ever reaches the continuous flow regime for the stresses that were tested.

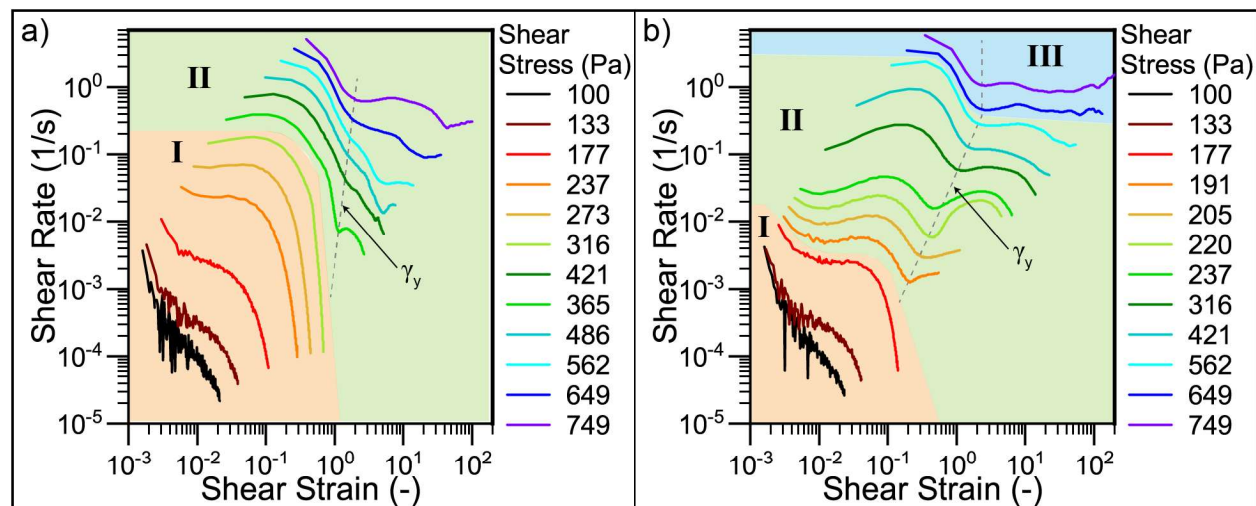


Figure 7: Transient creep results plotted as a function of shear strain for the a) base ink and b) 20 wt% PEO-PPO ink. Region I (orange) indicates the stress is below the yield stress. Region II (green) indicates the region where the inks show the re-entrant solid behavior. The stress is greater than the yield stress and less than the critical flow stress. Region III (blue) shows continuous flow after an initial yield event. The dashed lines indicate the yield shear strain ( $\gamma_y$ ). Within region II, the yield strain increases as a function of the stress. In region III, yield appears to occur at a consistent strain.

These observations seem to provide a rheological description for a problem in DIW that is colloquially described as “clogging”. It is often observed that for certain inks, the material flows consistently initially, but eventually stops flowing. According to our analysis, we would describe these printing pressures as sitting within the re-entrant solid regime for those inks – between the

<sup>3</sup> Landrum, B. J.; Russel, W. B.; Zia, R. N. Delayed Yield in Colloidal Gels: Creep, Flow, and Re-Entrant Solid Regimes. *J. Rheol.* (N. Y. N. Y). 2016.

yield stress and the flow stress. To test the relevance of the transient creep data to DIW, the ink mass flow through a DIW syringe and needle was measured over time for a variety of applied pressures. The results of these tests are shown in Figure 8. From these data, two key results can be observed. 1) Both inks had conditions in which the mass flow dropped as a function of time and stopped within a few minutes, consistent with the re-entrant solid regime. 2) The flow rate was higher for the 20 wt% PEO-PPO ink than the base ink for every pressure tested. These two results directly correspond to the results from the transient creep testing.

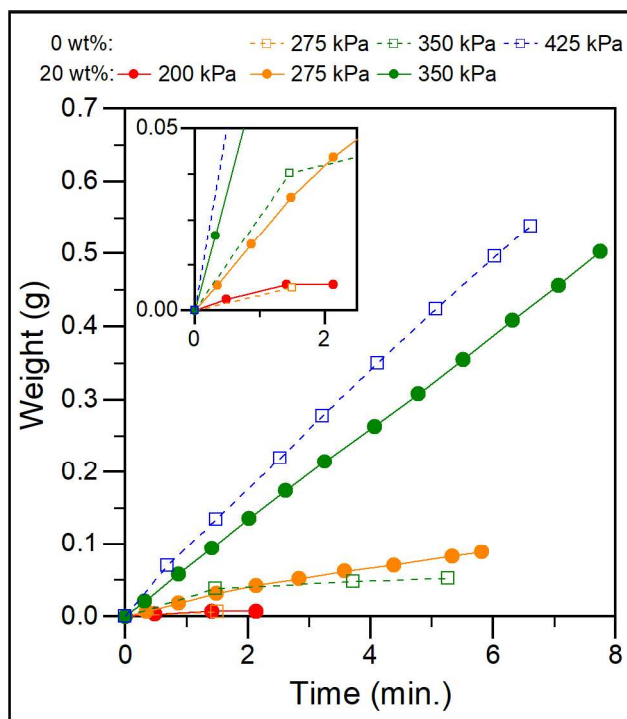


Figure 8: Printing flow vs time results for the base ink (dash line, empty square symbol) and the 20 wt% PEO-PPO ink (solid line, filled circle symbol). Tests were performed at pneumatic pressures of 200 kPa (red), 275 kPa (orange), 350 kPa (green) and 425 kPa (blue). Inset shows the low flow data points at early time points. Both inks had pressure conditions in which the flow stopped after short periods of time. The 20wt% PEO-PPO ink consistently flowed better than the base ink at comparable pressures.

We propose that the transient creep test is an important characterization test for DIW inks that may be more useful than other rheological protocols such as oscillatory testing. Creep testing can help identify any time or strain-dependent flow behaviors of a DIW ink. These results also show the importance of having a feedback control loop in DIW printers that monitor the flow rate, and can adjust pressures accordingly to maintain a consistent flow. This control loop is not currently available in most commercially available systems.

These studies have also shown that incorporation of the BCPs into these inks has actually improved the printability of the inks. The exact structural reason for this improvement is, as of yet, still unknown. One possibility is simply that the presence of the polymers helps promote exfoliation of the nanoclay during mixing. A more consistent nanoclay size would result in a decrease of the yield stress and more consistent flow. Another possibility is that the micelles provide a similar benefit to the nanoclay in that they can slide past one another during shear. In the future, we will want to perform more detailed in situ x-ray scattering experiments such as rheo-

SAXS and x-ray photon correlation spectroscopy (XPCS) to help determine what is happening structurally during ink flow.

### *Thermal Annealing of the BCP Structure*

The third primary effort of this project focused on studying the effects of thermal treatment on the material structure. One of the reasons why the base epoxy ink was chosen for this project was that the use of the EMIM-DCA crosslinker, instead of using a traditional amine, allowed for the crosslinking to be decoupled from the mixing. Here, the inks need to be heated to elevated temperatures in order for the epoxy to begin crosslinking. This allows us to easily print the materials at room temperature and store the material for days without worrying about the inks crosslinking and changing their properties. A second benefit is that we have the potential to use slightly elevated temperatures to initiate thermal annealing of the BCP structures in the inks before epoxy crosslinking. However, one potential problem that needed to be explored was to understand if the crosslinking mechanism would disrupt the BCP structures. Therefore, our effort in understanding the thermal effects was focused on answering two questions: 1) Can the samples be thermally annealed before crosslinking? 2) Is the structure retained during crosslinking? To answer both questions, a combination of SAXS and differential scanning calorimetry (DSC) were used. These studies were performed primarily with the PEO-PPO samples due to their availability. Additionally, if we can use thermal annealing to drive long range order, then this would become the preferred system.

DSC of the samples was first used to determine the temperature profile to use during the annealing and crosslinking steps. Uncured samples were first subjected to a heat-cool-heat cycle which extended to 250 °C at a temperature ramp rate of 25 °C/min. An example scan, containing 45 wt% block copolymer, 22% ionic liquid, and 33 wt% epoxy, is shown in Figure 9. On the first heating cycle, a strong exotherm ( $H = 252.6$  J/g) from the epoxy curing cycle is observed. A subsequent heating scan reveals no observable exotherm (data not shown), indicating the curing reaction is completed during the first heating scan. Next, an uncured sample was held at 100 °C for 4 hours to simulate the curing conditions during the in situ SAXS experiments. After the hold, the samples were cooled and heated again to determine whether there was another exotherm from the crosslinking of any unreacted material. The second heat profile is also shown in Figure 9c, and it can be clearly seen that there was no exotherm present, indicating that the reaction is essentially complete after 4 hours at 100 °C. Additionally, there was a desire to identify an elevated temperature in which the epoxy would not crosslink to determine whether there was any potential for thermally annealing the samples. DSC was again used to determine whether a hold at 60 °C for 4 hours would result in any epoxy cross-linking. The samples were held at 60 °C in the DSC for 4 hours before the samples were cooled to room temperature followed by heating through the epoxy crosslinking temperature. Exotherm analysis was again used to compare the heating cycles. The second heat ramp is shown in Figure 9b, and the total enthalpy was determined to be  $H = 253$  J/g. Therefore, it was determined that a hold at 60 °C for 4 hours resulted in virtually no epoxy crosslinking and could be used for future thermal annealing studies.

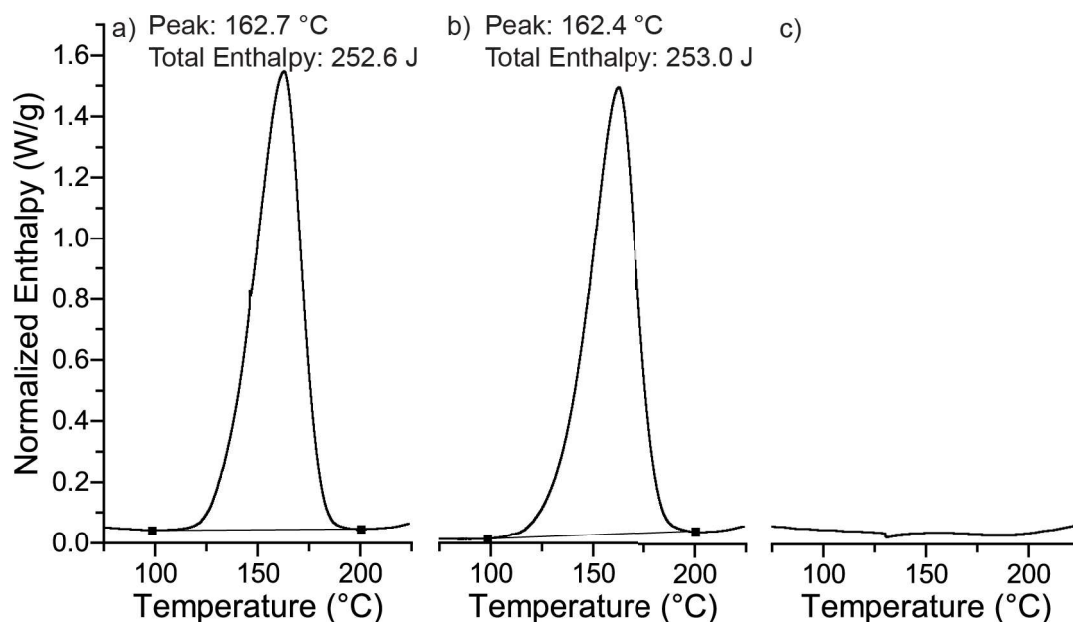


Figure 9: DSC heat scans of the 45 wt% PEO-PPO, 22% EMIM-DCA, and 33 wt% epoxy sample showing the normalized enthalpy during heating (25 °C/min) for samples that were a) never heated before the heat scan, b) annealed at 60 °C for 4 hours before the heat scan, and c) cross-linked at 100 °C for 4 hours before the heat scan.

The simplest experiment to determine the effect of crosslinking on the BCP structure consisted of measuring the SAXS of a composition before and after crosslinking. For these tests, the cured samples were loaded into the capillaries, then heated to 100 °C for 4 hours. The phase diagrams of the materials before and after crosslinking are shown in Figure 10. From these data, it can clearly be seen that many of the samples change their structure significantly during the crosslinking reaction. In general, for the conditions where the structure changes, we see a shift to a structure which we would expect for a composition with a higher BCP concentration (Figure 3). For example, disordered spheres at high epoxy concentration transition to BCC and Lam. Disordered sphere structures at the high EMIM-DCA and low PEO-PPO concentrations transition to Hex and Lam. The structures that were initially highly ordered seem to remain ordered after cross-linking. The shift in the stable phase to structures associated with higher polymer concentrations makes sense. As the epoxy crosslinks, the PEO blocks are likely being expelled from the vicinity of the epoxy. This results in a local concentration increase in the areas in which the micelles remain, likely triggering the change in structure. Additionally, since the EMIM-DCA is in excess for many of these compositions, a significant amount of the EMIM-DCA is still present in these regions with the BCP, thus continuing to provide the structure directing function. In future studies, we will be interested in performing transmission electron microscopy (TEM) on the samples to determine whether these structures still exist throughout the samples, or if then have formed microdomains of the self-assembled BCP that are separated from the epoxy network. Ideally, we would want the self-assembled domains to remain throughout the sample, and the epoxy network surrounding them and forming a continuous matrix.

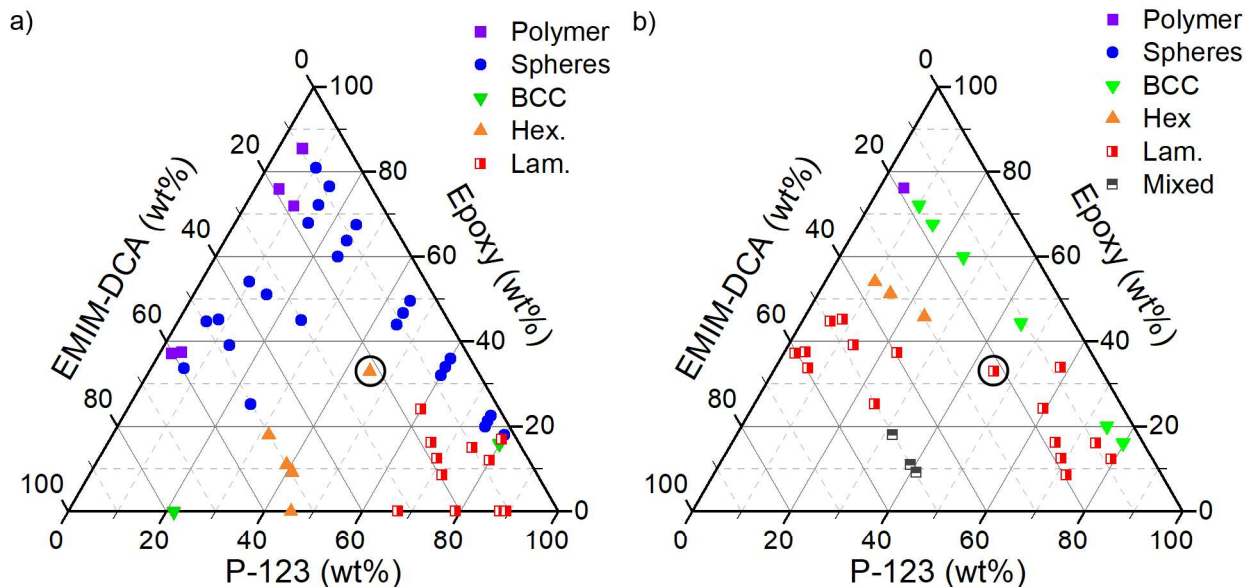


Figure 10: Ternary phase diagrams of the PEO-PPO (P-123) systems a) before and b) after curing. The sphere phase consistently converted to ordered phases during curing throughout the composition space. The circled composition was used for the DSC and the *in situ* SAXS studies.

To better understand what is happening during crosslinking, *in situ* SAXS was used to monitor the structure of the samples throughout the crosslinking reaction. However, these data in Figure 10 were collected on the SAXS line at Illinois, and required 30-60 minutes to collect enough scattering events to obtain quality results. Thus, the collection time was too long to obtain *in situ* data. Therefore, the *in situ* SAXS experiments were performed at the APS beamline 12-BM-B since quality data could be obtained over a measurement time of one minute. In these tests, the samples were held at 60 °C for 4 hours, quickly ramped to 100 °C, then held at 100 °C for 4 hours, and cooled back down to room temperature. The 1D linescans showing the scattering intensity ( $I$ ) versus the scattering wavelength ( $q$ ) were collected approximately every 5.75 minutes and are plotted for one sample as a function of time in Figure 11a. This sample (circled in Figure 10) was plotted here as it showed some of the most interesting changes of any of the samples. Additionally, it was of interest since it was the composition that had the highest epoxy concentration of any that showed ordered phases in the uncured state. The first peak in the SAXS can be related to the  $d$  spacing between planes of the phase-separated domains. Therefore, the  $d$  spacing are plotted in Figure 11b as a function of time to more easily monitor the changes in the structure. The ratios of the peaks determine the structure of the samples, and the structure is denoted by the symbol shape and color in Figure 11b.

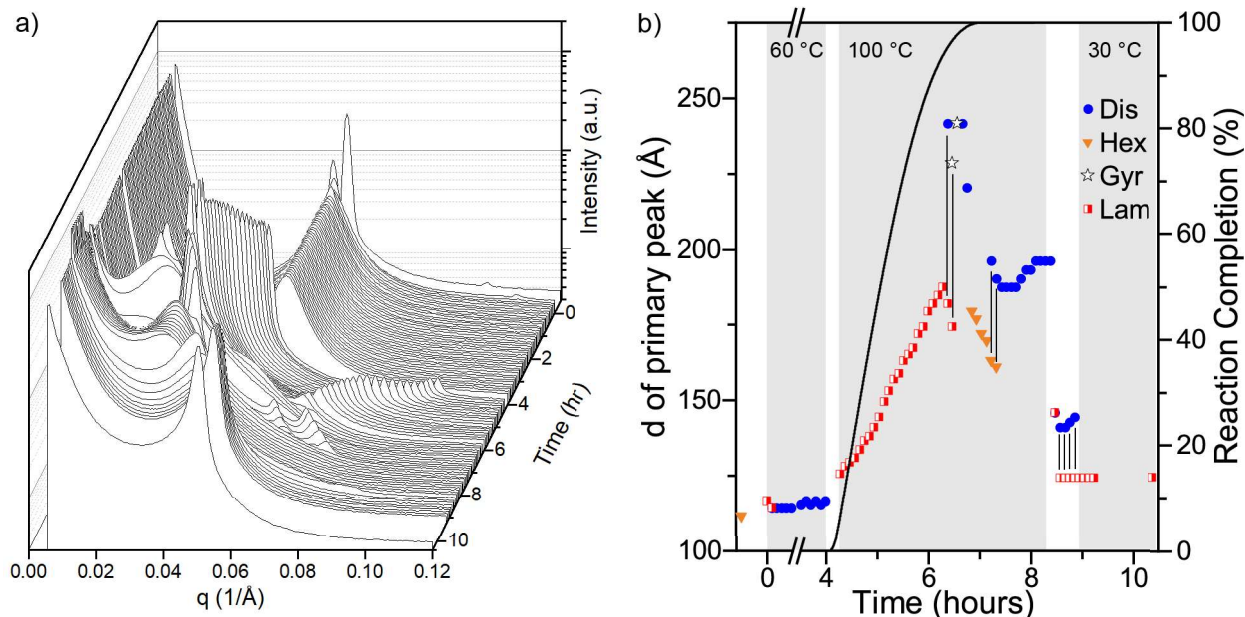


Figure 11: In situ SAXS data for a PEO-PPO BCP in epoxy/EMIM-DCA. Samples were held at 60 °C for 4 hours, then 100 °C for another 4 hours before being cooled down to room temperature. a) Linescans of the SAXS scattering through the entire experiment. b)  $d$  spacing of the BCP micelles as a function of the experiment time and the epoxy crosslinking completion by time as determined by DSC. The ink had a disordered structure throughout the majority of the 60 °C temperature hold, but then changed structures and spacing throughout the hold at 100 °C until settling on a lamellar structure with a spacing of 12.5 nm. Some SAXS data showed the co-existence of two phases at one time point, they are denoted in b) by two data points, with their respective structure and spacing, with a black vertical line between them to indicate the coexistence.

From these analysis, we can see that the  $d$  spacing does not change much within the first 4 hours, but the structure did transition from a Hex/Lam to a disordered structure at the beginning of the hold. The lack of changes in the  $d$  spacing indicates that the micelles very likely retain their local ordering (retain a roughly lamellar shape), but the long range order is lost due to the elevated temperature and the increased mobility of the polymers. Importantly, the micelles did not increase their order and thus it was concluded that they cannot be thermally annealed at 60 °C. However, as soon as the temperature is increased above 60 °C (> 4 hours), there are significant and immediate changes to the  $d$  spacing and the structure. The BCPs go from having a disordered structure to a lamellar structure. The  $d$  spacing continues to increase until at some time in the epoxy crosslinking when the gyroid structure begins to appear. Initially, there is a coexistence of a disordered phase with the lamellar until the gyroid phase fully appears. This indicates that this disordered phase is likely due to direct transition from the lamellar to the gyroid phase. The gyroid structure has the largest  $d$  spacing of any of these structures. At this point (~6.56 hours), the sample begins to transition to the Hex structure, through another transition disordered phase, while decreasing the  $d$  spacing. Eventually, the structure switches back to the disordered structure with an average  $d$  spacing of approximately 19 nm until the sample begins to be cooled back to 30 °C. Finally, once the sample has fully cooled, the lamellar structure stabilizes with a  $d$  spacing at approximately 12.5 nm. The 12.5 nm final  $d$  spacing is slightly larger than the initial  $d$  spacing of 11.5 nm. Taken together, these data help provide answers to the two primary questions for this effort.

Towards the potential for thermal annealing, the DSC data indicates that the epoxy crosslinking reaction does not occur appreciably during the thermal hold at 60 °C. However, this in situ SAXS data shows that the temperature was insufficient to thermally anneal the BCP structures.

The second question related to what happens to the BCP domains during epoxy crosslinking. The in situ SAXS data shows that there was a strong scattering peak for every time point measured. This indicates that the samples do not fully dissolve in the epoxy at elevated temperatures. In fact, it is fairly clear that the samples go through a disordered phase as they transition from one structure to another. If the BCP micelles had dissolved in the epoxy, they might not be very useful for our applications because that would mean that any encapsulated NPs would dissociate from the micelles and would have the potential to aggregate. However, the sample structures did change significantly throughout the heating process and even during the cool back to room temperature. The composition studied for the in situ work had a very low BADGE concentration (33 wt%), and thus it likely does not form a continuous epoxy network which is why we see structural changes even after the epoxy crosslinking has completed. However, the majority of the compositions that were characterized ex situ (Figure 10) showed changes in the structure. Taken together, these data show that the micelles do not completely break apart during the epoxy cross-linking, but the combination of the elevated temperatures and the epoxy cross-linking results in widespread structural rearrangement. Future studies will need to determine whether these structural changes could be predicted so that these changes can be accounted for in the design process.

In situ tests were also performed on several of the PI-PEO and PEP-PEO samples (Figure 12). Interestingly, these samples showed very little changes in the d spacing or the structure when exposed to the same heating cycle as those described with the PEO-PPO. Once again, thermal annealing (4 hours at 60 °C) did not seem to increase the extent of ordering, however, the fact that the micelles did not dissolve, change the structure or change their spacing was very encouraging. These polymers are clearly strong candidates for organizing NPs in the ink state, and retain that organization throughout the epoxy crosslinking reaction.

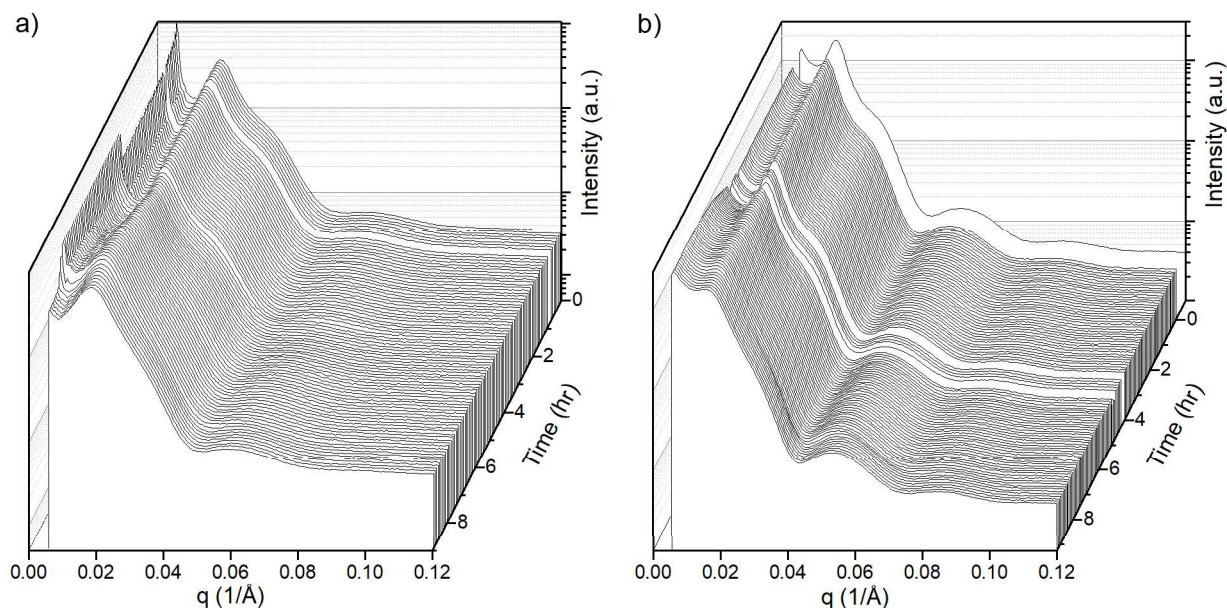


Figure 12: In situ SAXS of an a) PI-PEO and b) PEP-PEO sample during a 4 hour hold at 60 °C (0-4 h), a 20 minute ramp to 100 °C, a 4 hour hold at 100 °C (4.3-8.3 hours) and then cooled back to 30 °C.

## Conclusions and Future Directions

This effort has focused on studying the self-assembly, rheology and thermal characteristics of 3D printable block copolymer (BCP)-containing epoxy inks. Our original objective was that we could use a combined top-down, bottom-up approach to create hierarchical nanoparticles. While we have not yet accomplished this goal, we have made significant progress towards its achievement. We have identified three BCPs that form ordered structures in the epoxy/EMIM-DCA system. The PI-PEO and PEP-PEO were able to obtain ordered structures at low BCP and EMIM-DCA concentration, while the PEO-PPO required higher concentrations. These results establish that we can achieve the bottom-up assembly mechanisms. For the top-down portion, we needed to show that these systems can be printed through DIW. Our studies showed that not only are the BCP-containing epoxy ink printable, but their rheological properties are actually better than the base epoxy ink. This will allow us to print more consistently and at smaller filament diameters so as to provide the top-down assembly to lower length scales. Importantly, through these studies, we have identified creep testing as being a more informative rheological test than the more traditional oscillatory testing methods that are used in the literature. To help bridge the length scales between the bottom-up and top-down assemblies, we had hypothesized that the high shear during printing and thermal annealing during the epoxy curing can do this. Towards exploring this hypothesis, we used DSC and in situ SAXS to determine that while the epoxy do not crosslink at 60 °C, this temperature is insufficient for thermal annealing. Additionally, it was determined that many of the PEO-PPO materials do change their structure during the epoxy crosslinking reaction. However, in situ SAXS showed that these changes do not transition through a completely dissolved polymer phase, but rather through intermediate phase separated structures, which is important if the domains encapsulate nanoparticles. Interestingly, the PI-PEO and PEP-PEO materials showed very little change in the structure or the extent of ordering in the samples during the epoxy crosslinking. Through this study, we have investigated the basic structure/property relationships of these materials that we believe will serve as a critical springboard for future studies.

Future work from this effort will need to focus on further understanding the structure and dynamics of PI-PEO and PEP-PEO in epoxy inks in order to allow for the design of hierarchically ordered multifunctional nanocomposites. Specifically, we will need to make extensive use of in situ characterization of the materials during processing to understand the relevant length and time scales. This understanding will allow us to simultaneously design a materials system and processing method in which the relevant time and length scales are equivalent, thus enabling the formation of highly ordered printable inks. Imaging, specifically TEM, will be important to obtain a better understanding of extent of the assembled structures. Additionally, further analysis of the structural evolution of the BCP morphology using in situ SAXS as a function of thermal processing will continue. Another area that is ready for further in depth studies is in determining the structure and dynamics of the BCP/epoxy inks during flow (shear) through rheology, rheo-SAXS and x-ray photon correlation spectroscopy (XPCS). These studies could help us understand what happens to the BCP structures during shear, and the dynamics of the components in the ink during extrusion. Lastly, the effect of adding NPs to the inks on the structure and dynamics of the system will need to be studied. Increasing our understanding of what is happening to the components during thermal and shear processing will be critical to enable the development of a design paradigm for nanocomposites with ordered domains across 3D printed filaments that is informed by the fundamental structure-property relationships of the materials across several length scales.

## Metrics: Project Start to Date:

### Papers published and submitted:

1. Ekbote, R.P., Donley, G.J., Liu, D.Y., Rogers, S.A., Krogstad, D.K. "Re-entrant solid behavior of 3D-printable epoxy inks." *Rheo Acta* 2020, <https://doi.org/10.1007/s00397-020-01227-3>.
2. Liu, D.Y., Krogstad, D.K. "Phase Transformation of Nanostructured Block Copolymers in Ionic Liquid Cured Epoxy." To be submitted to *Macromolecules*.

### Presentations: \* denotes presenter

1. D.V. Krogstad\*. "Combined top-down and bottom-up approach in creating hierarchical order in organic based nanocomposites." 2017 AFOSR YIP Conference, Arlington, VA. Nov. 14, 2017.
2. D.V. Krogstad\*, D. Liu. "Using Block Copolymers as a Templating Additive to Create Ordered Polymer Nanocomposites." American Physical Society March Meeting, Los Angeles, CA. Mar. 9, 2018.
3. D.V. Krogstad\*. "Design and development of composites using additive manufacturing." Air Force Research Laboratory, Dayton, OH. Sep. 6, 2018.
4. R. Ekbote, D. Liu, G. Donley, S.A. Rogers, D.V. Krogstad\*. "Understanding the Effect of Block Copolymer Micelles in Inks for Direct Ink Writing." American Physical Society March Meeting, Boston, MA. Mar 5, 2019.
5. D. Liu\*, R. Ekbote, D.V. Krogstad. "Block Copolymer – Epoxy Blends for Additive Manufacturing." American Physical Society March Meeting, Boston, MA. Mar 6, 2019.
6. R. Ekbote, D. Liu, G. Donley, S.A. Rogers, D.V. Krogstad\*. "Effect of block copolymer micelles on the rheology of 3D printable epoxy inks." Society of Rheology Conference, Raleigh, NC. Oct. 24, 2019.

### Graduate Students Supported:

1. Deborah Liu (August 2017 – May 2020)

### Undergraduate Researchers Supported:

1. David Agapito (May-August 2017)
2. Deborah Liu (May-August 2017)
3. Rishabh Ekbote (May 2018 – May 2019)
4. Ryan Lin (May 2018 – May 2019)
5. David Johnson (May 2018 – December 2019)
6. Chris Miller (November 2018 – March 2019)
7. Katie Lee (May 2019 – August 2019)